Tensor low-energy electron diffraction



1994 J. Phys.: Condens. Matter 6 8103

(http://iopscience.iop.org/0953-8984/6/40/004)

J. Phys.: Condens. Matter 6 (1994) 8103–8132. Printed in the UK

REVIEW ARTICLE

# Tensor low-energy electron diffraction

P J Rous

Department of Physics, University of Maryland Baltimore County, Catonsville, MD 21228, USA

Received 28 June 1994

**Abstract.** The tensor low-energy electron diffraction (LEED) approximation is a perturbative approach to the calculation of LEED $I$ $V$ spectra. This article reviews the theory, applications and impact of the tensor LEED approximation upon surface crystallography by LEED. The theory of the tensor LEED approximation is outlined and the physical reasons for the success of the technique are discussed. Particular attention is paid to the relative importance of multiple scattering correlations in limiting the radius of convergence of the approximation. The applications and extensions of tensor LEED theory are reviewed. The utility of tensor LEED theory as the basis of novel methods in surface structure determination is outlined with particular emphasis upon the extension of tensor LEED theory to chemical and thermal displacements. The article concludes with a brief evaluation of future prospects and applications of the theory of tensor LEED.

## 1. Introduction

Over the past 20 years, the field of surface science has seen the continual development of new techniques for retrieving surface structural information and the associated claims of straightforward and routine interpretation of experimental data [1, 2]. The evolution of these techniques is described in a recent volume that reviews the first 30 years of surface science [3]. Yet, it can be argued that the pursuit of novel structural methods has obscured the steady experimental and theoretical development of the oldest surface structural technique; low-energy electron diffraction (LEED).

The birth of quantitative surface crystallography coincided with the first reports of surface structures solved by LEED that appeared in the literature in the early 1970s [4–6]. Since that time, the number of published surface structure determinations has risen steadily and a recent compilation of solved surface structures [7] contains almost 400 entries. Yet, despite the challenge of other structural methods such as ion scattering and scanning tunneling microscopy (STM), LEED accounts for approximately 70% of all solved surface structures and over 40% of all new structure determinations. The historic record demonstrates clearly that LEED remains the technique of choice for the retrieval of surface crystallographic information.

The last decade has seen important developments in both the theoretical and experimental components of the LEED technique. Whilst the experimental advances should not be underestimated [8], this review will focus upon one theoretical advance; the tensor LEED approximation. The tensor LEED (or TLEED) approximation has been the subject of an earlier review [9], which focused, in detail, upon the theory of the method and its early applications to specific surface structure determinations. Another recent tutorial [10] has reviewed the application of TLEED within the context of automated surface structure determination. This review will concentrate upon the basic physics of the tensor LEED

0953-8984/94/408103+30$19.50  

approximation and how the concept of tensor LEED has been used as the theoretical foundation for the development of novel approaches to surface crystallography such as chemical and thermal tensor LEED. This is one of the most important areas of development of the theory of tensor LEED over the last three years.

Although this review does contain a brief description the theory of tensor LEED (TLEED), more detailed expositions of the theory and the motivation behind its development can be found elsewhere [11–15]. It is not within the scope of this contribution to review the full dynamical theory in LEED. Instead, we refer the reader to several recent review articles [16–18] and books [19–22].

The organization of this review is as follows. In section 2 we briefly discuss the fundamental concepts necessary to understand surface structure determination by LEED. In section 3 we briefly describe the theory of linear tensor LEED and the more sophisticated version of the theory, tensor LEED. Also in section 3 we discuss the radius of convergence of the technique and the physical origins of the breakdown of the approximation. Particular emphasis is placed upon the classification of multiple scattering correlations. In section 4 we explore the efficiency of the tensor LEED approximation by examining its scaling behavior in comparison to full dynamical methods. Section 5 describes briefly how tensor LEED has been combined with various optimization strategies. In section 6, we tabulate the recent applications of tensor LEED to the solution of unknown surface structures. Section 7 reviews the ways in which tensor LEED theory has been used as the basis of novel techniques in surface crystallography by LEED.

## 2. Structure determination by LEED: basic concepts

All electron-based surface structural techniques achieve surface sensitivity by exploiting the short mean free path ($\lesssim 10$ Å) of low-energy electrons (30 to 500 eV) within solids [22], a consequence of strong inelastic scattering. Therefore, information retrieved from electrons *elastically* scattered from a solid must be sensitive to the local atomic arrangements at the selvedge. However, any realistic theory of electron scattering at surfaces, and certainly any theory capable of providing any degree of structural accuracy, must be capable of modeling the strong electron–atom scattering that occurs in this energy range. Typically, the electron scattering cross section of an atom seen by a low-energy electron is of the order of 1–10 Å$^2$. Since this value is similar to the physical cross-sectional area of an atom, *multiple* scattering among the surface atoms is expected to be of critical importance in determining the amplitude of the scattered electrons. Therefore, the extraction of structural information from the low-energy electron diffraction data requires an adequate theoretical model of the effect of multiple scattering.

For LEED, the structure determination employs a calculation of the propagation of electrons within the surface of a solid to extract the positions of the surface atoms from a set of measured intensity versus energy ($IV$) spectra corresponding to each Bragg beam diffracted from the surface. This procedure suffers from two computational bottlenecks that, until recently, greatly restricted the complexity of surfaces that could be investigated by the LEED technique. The first bottleneck was the amount of CPU time required to calculate the $IV$ spectra from a single trial surface structure for comparison with experiment. If we quantify the complexity of the surface structure by counting the number of inequivalent atoms within the surface unit cell, $N$, then the crudest summation of the multiple scattering paths takes an amount of time that scales as $N^3$. This cubic scaling is characteristic of the numerical matrix inversions needed to sum exactly the multiple scattering paths travelled by each scattered electron. These operations represent the dominant contribution to the total

CPU-time expended by a LEED calculation for a single surface structure.

The optimum scaling of the CPU time for a LEED calculation would be linear in $N$. This is the scaling exhibited by a kinematic calculation that neglects multiple scattering. However, single scattering is never a good approximation for LEED. Therefore, until the mid-1980s the bulk of the developments in LEED theory concentrated upon how to optimize the scaling of the CPU time for a single LEED calculation. This period saw the development of a number of reliable approximations to full multiple scattering [21], including renormalized forward scattering [22], reverse scattering perturbation [20–24], quasidynamical LEED [25–27], the beam set neglect method [21, 28] and the exploitation of symmetry [29].

At its inception in the mid-1980s, the tensor LEED approximation was a similar attempt at optimizing the scaling of a single LEED calculation. In fact, within its range of validity, the TLEED approximation can provide computational times that scale almost linearly with N. Although it was developed within this context, TLEED has had an important impact upon the second, and in many ways more serious, bottleneck in the LEED technique that occurs when the calculated LEED $IV$ spectra are compared to the measured spectra. This is the so-called structure search. Until the late 1980s, the optimum surface structure was selected by trial-and-error comparison of experimental and calculated spectra from a sequence of possible trial structures [21]. However, the time taken to perform an exhaustive search scales exponentially with the number of varied parameters, M (i.e. $t \propto C^M$). Consequently, as Pendry has indicated [30], the exhaustive LEED search belongs to the class of non-polynomial or NP-complete optimization problems for which the computational effort required to locate the structural solution is not bounded by a polynomial in M. As we shall demonstrate later in this review, even significant improvements in the speed of computer hardware have little impact on the size of NP-complete problems that can be solved by exhaustive searching. This problem has been alleviated by combining the tensor LEED approximation with automated optimization algorithms (ATLEED) and by extensions of tensor LEED theory such as linear LEED (LLEED).

Within this context, it should be noted that, whilst developments in digital computer hardware have increased both the computational cost-effectiveness and the convenience of LEED structure determination, hardware advances alone are responsible for only a relatively modest increase in degree of structural complexity of surface structures that can be solved by LEED. In a recent review, Duke [31] has pointed out that the (dollar) cost of a full dynamical solution of the GaAs(110)-p(1 × 1) surface has decreased by a factor of approximately 40 in the period between 1976 and 1992. Yet even such a dramatic increase in hardware efficiency leads to only a rather modest increase in the complexity of structures that can be solved because of the non-linear scaling of the dynamical LEED calculation with the number of atoms in the surface unit cell, $N$. If we assume that in 1976 a state of the art LEED calculation was for an elemental metal surface ($N = 1$), by 1992 hardware advances alone would allow us to solve surface structures with at most $N = 4$ atoms in the surface unit cell. This assumes that the dominant scaling behaviour of a LEED calculation is $N^3$, in reality the scaling of the entire structure search is much more unfavourable. In 1992 Van Hove *et al* published perhaps the most complex surface structure determination to date, Rh(1 1 1)-(2 × 2)-$C_2H_3$, a structure with no fewer than 31 determined parameters [32]. By waiting for hardware advances alone, this structure could not have been solved until approximately 2016! Instead this complex structure determination was made possible by advances in the theory of LEED and, in particular, the use of the tensor LEED approximation coupled with an automated search algorithm. This comparison demonstrates that the past and future advances in the complexity of LEED structure determinations lie in the development of new theories; not from a patient wait for advances in digital computer technology.

## 3. The theory of tensor LEED

### *3.1. Introduction*

Prior to the mid-1980s, and the development of the tensor LEED approximation, the majority of the successful approximation schemes in LEED could be classified as methods that neglected certain contributions to multiple scattering. In the kinematic limit, the CPU time required to compute the diffraction spectra, scales linearly with the number of inequivalent atoms in the surface unit cell. This is because the structure factor is simply a sum over phase factors; one for each atom. When multiple scattering is important, all possible propagation paths that link together the $N$ atoms must be summed to compute the total scattered amplitude. This is a numerical operation that scales as $N^3$. The success of approximation schemes developed prior to 1986 lay in the choice of a convergent partial summation over a sub-set of all the multiple scattering paths. For example, both RFS and RSP exploit the strong forward scattering of low-energy electrons by surface atoms to develop an expansion of the LEED amplitude truncated to low order in the number of backscattering events.

The conceptual foundation for tensor LEED theory is fundamentally different. Instead of developing an approximation to a full dynamical calculation for each trial surface structure, we attempted to develop a perturbation scheme that started with the results of a full dynamical calculation. The key motivation for tensor LEED was the realization that the most time-consuming part of any LEED structure determination is the evaluation of LEED $IV$ spectra, repeated perhaps hundreds of thousands of times, once for each trial surface structure that is compared to experiment. However, in most cases, each of these trial surface structures differed from one another by only small displacements of the surface atoms. What was needed was a computationally efficient means of re-evaluating LEED $IV$ spectra from distorted versions of a given surface structure, a task that was clearly suited to a perturbative approach.

### *3.2. Linear tensor LEED theory*

We start with a full-dynamical calculation for a particular surface structure called the reference structure. Since this reference calculation includes full multiple scattering corrections, it exhibits the usual, unfavourable, $N^3$ scaling of computational effort with the number of atoms in the surface unit cell. The reference calculation computes not only the $IV$ spectra but also the electron wavefunction within the reference surface, $\Psi_{k_\parallel}(r)$, that is produced by an incident beam of electrons with energy, $E$, and arbitrary momentum, $k_\parallel$, parallel to the surface. Since the muffin-tin approximation is used, the electron wavefunction in the interstitial region, just outside each surface atom, $r_j$, can be expressed as a spherical wave expansion,

$$\Psi_{k_\parallel}(r) = \sum_{\ell m} B_{\ell m}(k_\parallel)\left[j_\ell(\kappa|r - r_j|) + t_\ell h_\ell^1(\kappa|r - r_j|)\right] Y_{\ell m}(\hat{r}). \tag{3.1}$$

The spherical wave coefficients, $B_{\ell m}(k_\parallel)$, can be determined directly from the reference structure LEED calculation and $t_\ell$ is the usual atomic $t$-matrix.

We now consider how to approach the re-calculation of the IV spectra for a different trial structure where the atomic positions differ only slightly from those of the reference surface. The conventional approach would be to re-run the full dynamical calculation for the new set of atomic positions; an $N^3$ process. However, if the displacements of the atoms are, in some sense, small, then a perturbative approach can be taken. The most

elementary treatment, which is valid for the smallest displacements, computes the change of the potential generated by moving the $j$th atom through a distance $\delta r_j$:

$$\delta V_j \simeq \delta r_j \cdot \nabla V_j \tag{3.2}$$

where $\nabla V_j$ is the gradient of the surface potential evaluated at the position of the $j$th atom. A straightforward application of first-order perturbation theory yields the change in the amplitude, $\delta A$, of electrons scattered by the surface with parallel momentum $k_\parallel + g$:

$$\delta A_g(k_\parallel) \simeq \sum_j \langle \Psi_{k_\parallel+g} | \delta V_j | \Psi_{k_\parallel} \rangle \tag{3.3}$$

where $g$ is a reciprocal lattice vector corresponding to a particular Bragg reflection. Equation (3.3) may be evaluated by noting that

$$\langle \Psi_{k_\parallel+g} | r \rangle = \big( \langle r | \Psi_{k_\parallel+g} \rangle \big)^* = \langle r | \Psi_{-(k_\parallel+g)} \rangle \tag{3.4}$$

This is the electron wavefunction generated by an incident electron beam impinging upon the surface with parallel wavevector $-(k_\parallel + g)$. This quantity can be computed by performing a 'time-reversed' reference calculation for an incident electron beam parallel to $-(k_\parallel + g)$.

The matrix element of equation (3.3) can be evaluated in an angular momentum basis. The angular integral is straightforward, the radial integral can be expressed in terms of the atomic phase shifts of the atom that is displaced:

$$\int R^*_\ell(r) \frac{\mathrm{d}V(r)}{\mathrm{d}r} R_{\ell+1}(r) \mathrm{d}r = \exp[\mathrm{i}(\delta^a_{\ell+1} - \delta^a_\ell)] \sin(\delta^a_\ell - \delta^a_{\ell+1}).$$

This well known result originates from the theory of the electron–phonon interaction [33] and similar matrix elements to that of equation (3.3) are employed in the theory of phonon scattering in high-resolution electron energy-loss spectroscopy (HREELS) [34–36].

If we now combine equations (3.2) and (3.3) and consider the possibility of displacing $j = 1, \ldots N$, atoms, we find that the change in the amplitude of any LEED beam can be written as a sum over the three Cartesian coordinates of each atomic displacement ($i = x, y, z$):

$$\delta A_g \approx \sum_{j=1}^{N} \sum_{i=1}^{3} \mathcal{T}_{ij} \delta r_{ij} \tag{3.5}$$

where $\mathcal{T}$ is a Cartesian tensor:

$$\begin{aligned} \mathcal{T}_{1j} &= \mathcal{T}_{xj} = \langle \Psi_{k_\parallel+g} | \nabla_x V_j | \Psi_{k_\parallel} \rangle \\ \mathcal{T}_{2j} &= \mathcal{T}_{yj} = \langle \Psi_{k_\parallel+g} | \nabla_y V_j | \Psi_{k_\parallel} \rangle \\ \mathcal{T}_{3j} &= \mathcal{T}_{zj} = \langle \Psi_{k_\parallel+g} | \nabla_z V_j | \Psi_{k_\parallel} \rangle. \end{aligned} \tag{3.6}$$

The sum $i = 1$ to 3 is taken over the three Cartesian coordinates of each atomic displacement.

Equation (3.5) is the mathematical expression of the simplest version of the tensor LEED approximation called *linear tensor LEED*. It represents a highly efficient means of re-evaluating $IV$ spectra from (small) distortions of the reference structure. The reference calculation is needed to compute the tensor $\mathcal{T}$ including full dynamical corrections. However, once this is done, the LEED beam amplitudes and $IV$ spectra from a distortion of this surface can be rapidly evaluated by summing equation (3.5). This approach yields an approximate calculation of the $IV$ spectra for distortions of a reference structure at a rate that scales *linearly* with the number of atoms displaced; the optimum scaling for a LEED calculation. In practice the CPU time required for the trial structure calculations is negligible compared to that required for the reference surface.

### *3.3. The radius of convergence of linear tensor LEED*

Linear tensor LEED is, of course, only an approximation to a fully dynamical calculation. Consequently, we define a radius of convergence for the approximation: a length that represents the typical distance atoms may be displaced from their positions in the reference surface whilst retaining sufficient accuracy to determine the atomic positions within the error bars of a LEED analysis (typically $\pm 0.05$ Å). Using this definition we anticipate that the results of a fully dynamical and a TLEED analysis of a given surface structure will agree within the error bars of the analysis, provided atoms are not moved outside of the radius of convergence of the TLEED approximation. Note that this definition does not imply that the $IV$ spectra calculated by TLEED are identical to those computed by full dynamical calculation. Instead this definition implies that there is no loss of structural information when the TLEED approximation is used within its radius of convergence.

There are two assumptions made by linear TLEED that lead to a finite radius of convergence. First, we have made the assumption that the change in the potential, $\delta V$, and the change in the LEED amplitude, $\delta A$, are accurately represented as a Taylor series expansion truncated at first order in $\delta r$:

$$\delta V_j \simeq \delta r_j \cdot \nabla V_j + \mathrm{O}\left(\delta r_j^2\right). \tag{3.7}$$

This is true only if the displacement $\delta r$ is sufficiently small. Since this is an approximation to the local perturbing potential, its validity is independent of the degree of multiple scattering. Consequently, a kinematic model suffices to estimate how well the changes in the LEED amplitudes are represented by the linear TLEED approximation for the potential.

Consider a small displacement, $\delta r$, of a single atom, form factor $f$, in the single scattering limit. The change in the scattered amplitude corresponding to momentum transfer $(k - k')$ is

$$\delta A = f \exp[(k-k')\cdot(r+\delta r)] - f\exp[(k-k')\cdot r] \simeq \left[(k-k')\cdot\delta r + \mathrm{O}(\delta r^2)\cdots\right]. \tag{3.8}$$

This linear expansion fails when $(k-k')\cdot\delta r \leqslant 2\kappa\delta r$ becomes significant compared to unity. It follows that, for a typical set of normal-incidence $IV$ spectra where $30 \leqslant E \leqslant 300$ eV and $|(k-k')| \approx 2\kappa$, the largest displacement is limited to $\delta r \lesssim 0.35$ Å at 30 eV and $\delta r \lesssim 0.10$ Å at 300 eV. This suggests that the radius of convergence of the linear tensor LEED approximation is not greater than approximately 0.1Å. Further, it is interesting to note that the validity of the linear tensor LEED approximation depends not only upon the change of the on-site potential but also upon the momentum transfer corresponding to the diffraction of the LEED beam. This is consistent with the interpretation of the RHS of equation (3.3) offered by the Hellmann–Feynman theorem; it is proportional to the force exerted on the undisplaced atom by the electrons scattered along $k_{\|} + g$.

The second approximation made by the linear tensor LEED approximation is the assumption that an electron does not experience the perturbation of the potential produced by any displaced atom more than once. This implies that, in linear tensor LEED, the multiple scattering paths are summed to all orders in the $V_j$ but only to first order in $\delta V_j$. In other words, the change in potential is sufficiently small that contributions to $\delta A$ from terms containing products such as $\delta V_j \delta V_k$, can be neglected in this version of TLEED. The validity of this assumption requires that the perturbing potential at each atomic site is so small that there is negligible multiple scattering between the $\delta V_j$. Since, at LEED energies, strong multiple scattering occurs between the full atomic potentials $V_j$, a necessary condition for the validity of linear TLEED is that $\delta V_j \ll V_j$. Note that, in the kinematic limit, this

approximation becomes exact and therefore the only limitation is the representation of the perturbation of the scattering potential.

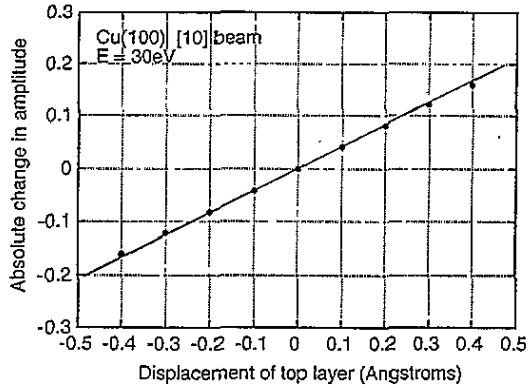


**Figure 1.** The absolute change in amplitude, $|\delta A|$, of the [1 0] beam scattered from a Cu(1 0 0) surface for an incident electron energy of 30 eV. The change in amplitude (•) is shown as a function of the displacement of the entire top layer of atoms with respect to the layer position in the bulk termination of the solid. Negative values of $d$ correspond to a contraction of the first interlayer spacing. The electron beam was incident normal to the surface.

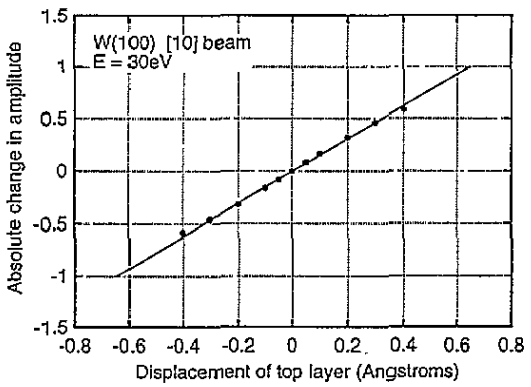


**Figure 2.** The absolute change in amplitude, $|\delta A|$, of the [1 0] beam scattered from a W(1 0 0) surface for an incident electron energy of 30 eV. The change in amplitude (•) is shown as a function of the displacement of the entire top layer of atoms with respect to the layer position in the bulk termination of the solid. Negative values of $d$ correspond to a contraction of the first interlayer spacing. The electron beam was incident normal to the surface.

Failure of either of these approximations will cause the change of amplitude, equation (3.3), to deviate from its linear dependence upon the atomic displacements. Consequently, the validity of the linear version of TLEED may be explored by computing the change of amplitude including full dynamical corrections and looking for deviations from linearity as a function of the magnitude of an atomic displacement. Figures 1, 2 and 3 show the change in scattered amplitude, $\delta A$, evaluated as a function of the distance $d$ that the top layer of atoms was displaced into and out of several clean, elemental, surfaces. Results are shown for incident electron energies of 30 eV for Cu(1 0 0) and W(1 0 0), and 200 eV for Ni(1 0 0). For both Cu(1 0 0) and W(1 0 0) at 30 eV, it is clear from figures 1 and 2 that the change in amplitude $\delta A$ is linear in the planar displacement, $d$, for distances smaller than 0.4 Å. At 200 eV, the results for Ni(1 0 0) in figure 3, also show linear behaviour but

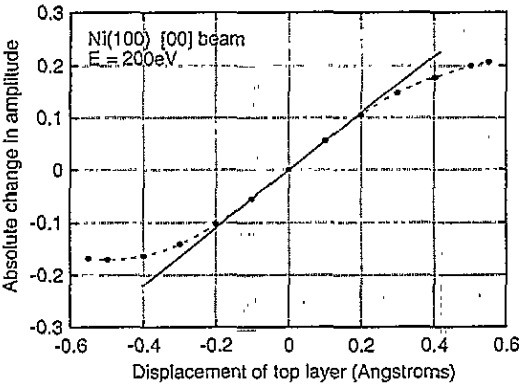


**Figure 3.** The absolute change in amplitude, $|\delta A|$, of the [00] beam scattered from a Ni(1 0 0) surface for an incident electron energy of 200 eV. The change in amplitude (•) is shown as a function of the displacement of the entire top layer of atoms with respect to the layer position in the bulk termination of the solid. Negative values of $d$ correspond to a contraction of the first interlayer spacing. The electron beam was incident normal to the surface. Note the linear dependence of the change in amplitude upon the displacement for $d \leqslant 0.2$ Å.

for a smaller range of displacements, less than about $d = 0.2$ Å. These upper limits of the magnitudes of the atomic displacements are quantitatively consistent with the magnitudes predicted for the failure of the linear representation of the potential, discussed earlier in this section.

Further evidence for the failure of the description of the potential being the cause of the breakdown of the linear TLEED approximation may be seen by comparing the W(1 0 0) and Cu(1 0 0) examples for an incident electron energy of 30 eV. It is well known that W is an extremely strong scatterer of LEED electrons, especially at low energies. The calculated scattering cross section of W at 30 eV is $\sigma_W \approx 5.6\,\text{Å}^2$ compared to $\sigma_{Cu} \approx 0.5\,\text{Å}^2$. Thus at 30 eV we expect significantly greater multiple electron scattering in W(1 0 0) than in Cu(1 0 0). Consequently, if multiple scattering correlations were the limiting factor for the linear tensor LEED approximation, then the radius of convergence for W(1 0 0) should be significantly smaller than for Cu(1 0 0) at 30 eV. Since this is not the case, we conclude that multiple scattering correlations between displaced atoms are not the limiting factor in the *linear* TLEED approximation. The physical reasons for the relative unimportance of multiple scattering correlations will be discussed later in this review.

### *3.4. Tensor LEED theory*

Our analysis of the failure of linear TLEED suggests that the radius of convergence of the approximation could be extended by improving the on-site representation of electron scattering by a displaced atom. This more sophisticated approach, called simply TLEED, is outlined in this section.

In linear TLEED the perturbation of the potential corresponding to a single atom, caused by a displacement $\delta r$, is evaluated approximately by taking only the first order term in the Taylor expansion of the distorted potential. Instead, the effect of this perturbation upon the electron scattering at a single atomic site may be evaluated exactly, at least within the rigid muffin-tin approximation. Rather than considering the change in the potential we compute the change in the scattering $t$-matrix of the displaced atom. To do this we employ an angular momentum basis and use the translation theorem for spherical waves.

Consider the scattering $t$-matrix of an atom situated at the origin. This quantity may be

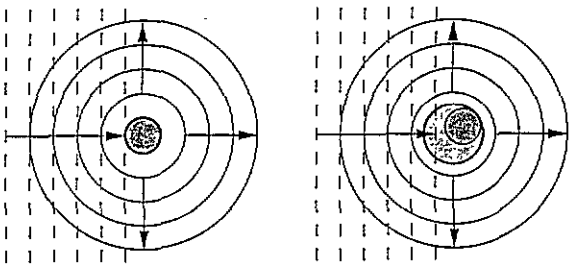

**Figure 4.** A schematic illustration of how the displacement of an atom can be considered as a distortion of the atomic scattering matrix. The left panel shows an incident plane wave scattered into a spherical wave originating at the centre of an atom. The right panel shows how the scattering by a displaced atom can be expressed in terms of spherical waves centred upon the original position of the atom.

expressed in terms of the usual scattering phase shifts $\delta_\ell$:

$$t_\ell = \mathrm{i}\exp(\mathrm{i}\delta_\ell)\sin\delta_\ell. \tag{3.9}$$

If the atom is displaced then either we can use this $t$-matrix at the new position of the atom, or we can incorporate the effect of the displacement directly into the atomic $t$-matrix.

$$\hat{t} = t + \delta t(\delta r). \tag{3.10}$$

It should be understood that the perturbed $t$-matrix is referenced to the undisplaced position of the atom (i.e. the origin). From the point of view of the electron scattering states, this approach is advantageous because the origin of the spherical wave expansion of electron wavefunction in the vicinity of the atom remains unaltered when the atom is moved. Instead the atomic displacement introduces off-diagonal elements into the $t$-matrix that now represents the non-central potential of the displaced atom. This is illustrated schematically in figure 4.

In an angular momentum basis, $\delta t$ can be computed for each displaced atom in the reference surface by using the translation theorem for spherical waves [37]. Then, the change of the amplitude of the LEED beam diffracted with parallel wavevector $k_\parallel$ is obtained by replacing equation (3.3) with

$$\delta A_g = \sum_j \langle \Psi_{k_\parallel+g} | \delta t_j | \Psi_{k_\parallel} \rangle. \tag{3.11}$$

Inserting a complete set of angular momentum states $\langle \ell m|$ on either side of the $\delta t_j$ in equation (3.11), we find the analogous expression to equation (3.3) for the change in scattered amplitude:

$$\delta A_g = \sum_j \sum_{\ell m, \ell' m'} \mathcal{T}^j_{\ell m, \ell' m'} \delta t^j_{\ell m, \ell' m'}. \tag{3.12}$$

This expression is correct to all orders of $\delta r$ since $\delta t_j$ represents the exact change in the on-site potential produced by displacing the $j$th atom.

It is instructive to compare the change in the scattered amplitude calculated using the linear TLEED approximation, equation (3.3), and using the TLEED approximation equation (3.12). In the linear approximation, the change in the amplitude is the product of a tensor and the actual atomic displacement, summed over the three Cartesian coordinates and the displaced atoms. In the more sophisticated version of the theory, equation (3.12), the amplitude change is the product of a tensor with the change in the on-site $t$-matrix, summed over all angular momentum components and over all of the displaced atoms. The

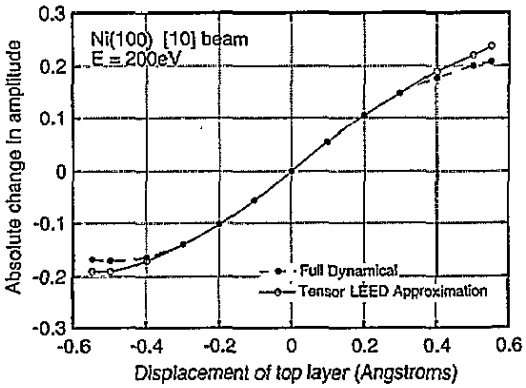


**Figure 5.** The absolute change in amplitude, $|\delta A|$, of the [1 0] beam scattered from a Ni(1 0 0) surface for an incident electron energy of 200 eV. The change in amplitude is shown as a function of the displacement of the entire top layer of atoms with respect to the layer position in the bulk termination of the solid. Full dynamical calculation (•) and TLEED approximation are shown (O).

link between the first and second versions of the TLEED approximation can be established by substituting into equation (3.11) the expression for $\delta t^j$ evaluated in the first Born approximation; $\delta t^j = G_0^+ \delta V^j G_0^+$, thereby yielding equation (3.5).

In both versions of the TLEED approximation, the tensor $\mathcal{T}$ depends only upon the properties of the reference surface. In the more sophisticated version of the TLEED approximation, the atomic displacements, $\delta r_j$ do not appear explicitly in the formula for the change of amplitude. Instead, the $\delta t$ are functions of the atomic displacements. Nevertheless, once the reference structure calculation has been performed, it is only necessary to recalculate the $\delta t$ for each trial structure. Whilst it is obvious that the evaluation of the $\delta t$ is more a computationally costly procedure than the calculation of the atomic displacements, the scaling of this version of the approximation is still linear in the number of displaced atoms.

Figure 5 shows a comparison of the more sophisticated version of the TLEED approximation and a full-dynamical LEED calculation for an example discussed in the previous section, Ni(1 0 0) for an incident electron energy of 200 eV (see figure 3). In figure 5, the change in the scattered amplitude, $\delta A$, was evaluated as a function of the displacement of atoms into and out of the top Ni layer. Clearly, even at 200 eV, the TLEED approximation accurately reproduces the change in amplitude for atomic displacements as large as 0.4 Å. Thus it is apparent that the second version of TLEED extends the validity of the approximation significantly beyond that of linear tensor LEED.

### *3.5. The radius of convergence of the TLEED approximation*

The radius of convergence of TLEED has been determined empirically from applications of the technique to the analysis of actual LEED data. There have been numerous comparisons between full-dynamical and TLEED calculations of IV spectra for many different surface structures [11, 13, 38, 39]. The reader is referred to the published structure determinations listed in table 1 (section 6) that contain specific examples of the applications of TLEED. In this section, we will confine the discussion to analysis of the physical reasons for the success of the approximation and its limitations.

For atomic displacements outside its radius of convergence, the more sophisticated version of TLEED breaks down. In the case of *linear* TLEED, the breakdown of the method

was attributed to a failure of the approximation to describe correctly the potential of the displaced atom. This cannot be the reason for the failure of the TLEED approximation, since the change in potential is represented exactly provided the change in the atomic $t$-matrix is calculated accurately. As an aside, it is useful to clarify at this stage of the discussion what is meant by an exact evaluation of $\delta t$. This is because, in reality, some approximations are made in the evaluation of this quantity. However, we shall see that these approximations do not play a role in determining the radius of convergence of TLEED.

First, when evaluating $\delta t$ we employ the rigid muffin-tin approximation (RMTA) and displace the entire muffin-tin potential of an atom to its position in the trial surface. Compared to a fully self-consistent calculation of the atomic scattering, the RMTA is an approximation since displacing the atom alters the valence electronic charge density in its vicinity. However, all state-of-the-art full dynamical LEED calculations employ atomic phase shifts derived from bulk or cluster calculations and take no account of the change of atomic scattering as the atom is moved within the surface. Consequently, although the use of the rigid muffin-tin approximation is an approximation to the true surface potential, it is an approximation that is also made by full dynamical calculations for the same surface structure. The only circumstance where problems can arise is when there is significant overlap of the muffin-tin potentials of nearest-neighbour atoms, caused by displacing one atom in the reference surface towards another. In this case, either the muffin-tin radius of the atom in the reference surface must be adjusted, or a new reference structure chosen that is more closely related to the trial structure.

The second approximation made in the calculation of $\delta t$ is the truncation of the angular momentum expansion used to represent the quantity. A typical LEED calculation employs sufficient ($\ell m$) values to describe accurately the atomic scattering. Typically, one uses a semi-classical rule of thumb, $\ell_{\max} \geqslant \sqrt{2E}R$, where $R$ is the muffin-tin radius of the atom. When the atom is displaced by an amount $\delta r$, the perturbed $t$-matrix $t+\delta t$ now represents a region of scattering that is slightly larger than that of the undisplaced atom. Consequently, a slightly larger number of angular momentum components are needed to describe the scattering from the displaced atom. Since in all LEED calculations $\ell_{\max}$ is fixed at an energy independent value, the effect of the truncation of the angular momentum expansion used to represent $\delta t$ is most apparent at high electron energies. Consequently, when TLEED is employed, care must be taken to include a sufficiently large angular momentum basis to treat the largest displacements. Provided this is done, the atomic scattering in the trial surface is represented as accurately as that of atoms in the reference structure.

If these precautions are taken, then the origin of the failure of the TLEED approximation is the appearance of multiple scattering correlations between displaced atoms. As the change in $t$-matrix, $\delta t$, becomes significant in comparison to the full atomic $t$-matrix, multiple scattering between displaced atoms begins to make a significant contribution to the scattered intensity.

The importance of multiple scattering correlations can be seen by considering the multiple scattering paths contributing to the scattered intensity. In the reference surface the propagation of an electron between an atom pair $(i, j)$ can be represented by the full Green function $G^r_{ij}$ for the reference surface:

$$G^r_{ij} = G^0_{ij} + \sum_k G^0_{ik} V_k G^0_{kj} + \sum_k \sum_\ell G^0_{ik} V_k G^0_{k\ell} V_\ell G^0_{\ell j} + \cdots . \tag{3.13}$$

Here $G^0_{ij}$ is the free-space Green function that describes the free propagation of LEED electrons within the reference surface from atom $i$ to atom $j$. Since a full dynamical calculation is performed for the reference surface, the full Green function linking every

atom pair is computed exactly, i.e. equation 3.13 is summed to all orders in $V$. This must be done because the strength of the atomic potentials $V_j$ means that this series cannot be truncated at a low order in $V$.

We now consider a trial surface where some atoms have been displaced from their positions in the reference structure. The full Green function for the trial surface is

$$G^t_{ij} = G^r_{ij} + \Delta G_{ij} \tag{3.14}$$

where

$$\Delta G_{ij} = \sum_k G^r_{ik}\delta V_k G^r_{kj} + \sum_k \sum_\ell G^r_{ik}\delta V_k G^r_{k\ell}\delta V_\ell G^r_{\ell j} + \cdots. \tag{3.15}$$

Although the multiple scattering series for $G^r_{ij}$ must be summed exactly, the series for $\Delta G_{ij}$ can be truncated if $\delta V$ is sufficiently small compared to $V$. In the TLEED approximation, $\Delta G_{ij}$ is summed only to first order in $\delta V$:

$$\Delta G_{ij} \simeq \sum_k G^r_{ik}\delta V_k G^r_{kj} + O(\delta V^2) + \cdots. \tag{3.16}$$

This approximation will fail, and the radius of convergence will be reached, when $\delta V$ becomes so large that higher-order terms in equation (3.16) become significant.

Physically, these higher-order terms in the multiple scattering expansion for $\Delta G_{ij}$ may be classified into two types: those paths on which an electron returns to the same displaced atom more than once (closed paths) and those that do not (open paths). A schematic illustration of these multiple scattering paths can be seen in figure 6. It can be argued that contributions to the scattered intensity from scattering paths on which an electron returns to the same displaced atom more than once are of significantly less importance than open paths. This is because closed loops represent a small proportion of the total number of possible scattering paths and on such paths an electron must undergo backscattering from the atoms surrounding the displaced atom. At LEED energies, backscattering is a weak process compared to forward scattering by atoms, an argument that is used to justify the neglect of multiple scattering correlations between displaced atoms in the theoretical treatment of lattice vibrations in LEED [22] and disordered alloys [40]. Consequently, we argue that the radius of convergence of the TLEED approximation is largely determined by its failure to represent correctly multiple scattering correlations between displaced atoms and, in particular, the open scattering paths on which electrons are scattered by two distinct displaced atoms.

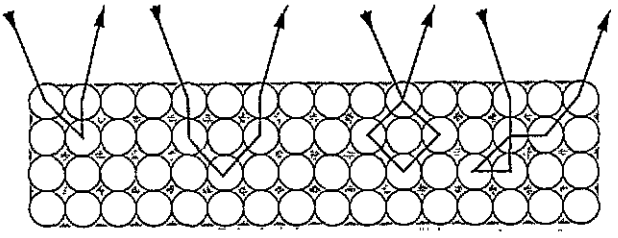


**Figure 6.** A schematic illustration of the multiple scattering paths within a trial surface. These paths are classified into open paths of the type shown in the left panel and closed paths shown in the right panel.

Our analysis of the origin of the failure of TLEED allows us to understand the variation of the radius of convergence between different surfaces. Early applications of TLEED showed

that the radius of convergence was approximately 0.4 Å for elemental surfaces such as Ni and Cu. However, it should be recognized that this is not a universal value. Since the magnitude of $\delta V$ for a displaced atom is dependent upon the strength of the (unperturbed) atomic potential, we expect a correlation between the scattering cross section of a surface atom and the radius of convergence of TLEED when it is used to displace the atom. This is what is found empirically. For materials in the middle of the periodic table, such as Ni, Cu, Pd, Mo and Rh, the radius of convergence is found to be close to this value, 0.4 Å . However for heavier materials, such as W, the radius of convergence shrinks to approximately 0.3 Å . For Pt it is closer to 0.2 Å . By contrast, for lighter atoms, such as C, N, O and H, the radius of convergence expands beyond 0.5 Å . These results are consistent with an inverse relationship between the scattering cross section of the atom and the radius of convergence of the TLEED approximation. This follows from the general, albeit non-monotonic, increase in the atomic scattering cross section with atomic number as one descends the periodic table.

In addition to being correlated with the strength of the atomic scattering, the importance of open multiple scattering paths in limiting the radius of convergence of the approximation implies that the success of TLEED for a particular surface structure should also depend on the relative position of displaced atoms. The radii of convergence quoted above are for the (worst) cases where TLEED was used to consider multilayer relaxations where all the atoms in a single atomic plane are moved in concert. In these cases the displaced atoms are nearest neighbours and multiple scattering correlations between displaced atoms are maximized.

If displaced atoms are further apart than the electron mean free path, then multiple scattering correlations between these atoms will never become significant. In this case, the approximation fails only when there is significant multiple (back)scattering along closed paths that link the same atom. Because of the relative unimportance of these closed paths compared to the open paths, we anticipate that the radius of convergence of TLEED is extended when displaced atoms are far apart. Further, if the (back)scattering correlations could be included in the perturbation series then, when displaced atoms are far apart, the approximation could remain valid for significantly larger displacements than TLEED. These backscattering paths are included in the linear LEED method recently proposed by Wander *et al* [41]. Linear LEED, and its relationship to TLEED will be discussed in section 7.2.

## 4. The efficiency of tensor LEED

The fundamental advance offered by TLEED theory, in either of its implementations, is that, once a reference structure calculation has been performed, the CPU time required to evaluate $IV$ spectra from a trial surface structure scales *linearly* with the number of displaced atoms. Thus, if we compare the CPU time required for a TLEED ($\propto N$) and a full dynamical calculation ($\propto N^3$), we expect a reduction in CPU time of at least a factor of $N^2$. This is very significant time-saving even if TLEED is used to move only a few atoms. Further, the simplicity of the numerical operations required to compute the $IV$ spectra from distortions of the reference surface means that the TLEED calculation is very fast compared to conventional full dynamical methods. For example, by using TLEED theory the CPU time expended per trial structure can be reduced by a factor of 50 for simple elemental surfaces such as Cu(1 0 0), even though $N = 1$ in this case.

However, even this analysis of the efficiency of the method greatly underestimates the potential time savings offered by TLEED when it is applied to complex surfaces. In contrast to conventional LEED calculations that exploit time-saving symmetries, the time taken to evaluate intensities by TLEED is independent of the degree of symmetry within any given

trial structure. One can consider highly asymmetric systems with no loss of efficiency. Therefore, it is possible to select a reference structure that is highly symmetric (and may be efficiently treated by full dynamical methods) and then use TLEED to distort this surface into a structure that possesses significantly fewer symmetry elements.

If only a few trial structures are considered, the CPU time required for the entire structure determination will be dominated by the $N^3$ scaling of the reference structure calculation. However, except for the simplest elemental surfaces, most structure determinations investigate a very large number of trial surface structures (often several hundred thousand structures). In these cases, the scaling of the CPU time is dominated by the time taken to perform the trial structure calculations, which scales linearly with the number of displaced atoms. In these cases, the TLEED approximation has optimized the scaling of the time taken to perform the LEED calculations for each trial structure. Whilst this removes the first computational bottleneck discussed in section 2, it leaves the other in place: the exponential scaling of the number of trial structures needed to perform a trial and error search of parameter space. This difficulty has been overcome by combining TLEED with automated search strategies and is discussed in the next section.

## 5. TLEED and automated search strategies

### *5.1. Introduction*

The use of automated search algorithms has been the subject of a recent review [10], and the various optimization methods will not be discussed in detail here. Instead we will confine the discussion to the motivation for and development of such methods using TLEED.

The search problem in surface crystallography by (LEED) may be stated concisely as follows: given a set of experimental $IV$ spectra and a means of calculating $IV$ spectra from any trial surface structure, how does one determine the actual surface structure? Typically, one proceeds by using an R-factor that measures the mismatch between the experimental and calculated $IV$ spectra for each trial surface structure [21]. One then employs a search strategy to find the set of structural and non-structural parameters that minimizes the disagreement between the calculated and measured $IV$ spectra. This approach transforms the crystallographic determination into the standard numerical optimization problem of locating the global minimum of a multi-dimensional $R$-factor hypersurface that spans the parameter space formed by the structural and non-structural variables.

The time taken to perform such an exhaustive search of parameter space scales exponentially with the number of varied parameters, $M$. Consequently, even significant improvements in the speed of computer hardware make little impact on the size of NP complete problem that can be solved by exhaustive searching. For example, as was noted in the introduction, the cost of the LEED structure determination for GaAs(110) ($M \simeq 8$) in 1992, \$40, has decreased by a factor of 40 in the period between 1976 and 1992. If we extrapolate this example to the case of the Rh(1 1 1)-(2 × 2)-$C_2H_3$ ($M \simeq 30$) surface considered earlier, then we find that the cost for the solution of this structure is no less than \$1,000,000. This is a consequence of the exponential scaling of CPU time/cost with the number of fitted parameters.

### *5.2. Local and global search methods*

Over the last five years, there have been several applications of local directed search methods to the LEED structure search [10, 42–45]. These methods improve the efficiency

of the structure search by exploiting the local topography of the $R$-factor hypersurface. These techniques are fully or partially based upon descent methods and attempt to convert the $M$-dimensional search into a sequence of $M$ one-dimensional line searches. Cowell *et al* implemented the first gradient search method using full-dynamical calculations of $IV$ spectra for comparison with experiment [42]. The Munich group has implemented a gradient-expansion method using fully dynamical calculations [43, 44].

The TLEED approximation has been combined with a local search method to explore rapidly the $R$-factor hypersurface in the vicinity of a reference structure [45]. All directed searches are launched from an initial point in parameter space and find the minimum of the cost function that is, in some sense, closest to the starting point. Clearly, TLEED is compatible with this type of search, since the search can be launched from the point in parameter space that corresponds to a reference structure and confined to a local region of parameter space within the radius of convergence of the approximation. Therefore it is possible to exploit the efficiency of both TLEED and the automated searching simultaneously.

The automated TLEED (ATLEED) approach is illustrated in the flowchart of figure 7. The first program generates, and then stores to disk file, one tensor $\mathcal{T}$ for each energy point, for each observed beam and for each atom to be displaced from its reference position. The second program reads those tensors and calculates LEED $IV$ spectra for a sequence of trial structures using the TLEED approximation. The $IV$ spectra of each trial structure examined are immediately compared to the experimental spectra by an *in situ* $R$-factor calculation. A steepest descent method is used to choose the next trial structure from the results of the previous $R$-factor comparison. This procedure is repeated until the search converges at an $R$-factor minimum.

This type of optimization procedure does not guarantee that the trial structure at the termination of the search is the best-fit surface structure: this structure may correspond to a local and not the global $R$-factor minimum. A heuristic, and oft-recommended, solution to the problem of global versus local minima is to launch multiple directed searches from different initial structures [10, 45]. Using this approach, it is hoped that all $R$-factor minima are located and therefore the global minimum may be selected from this list of minima. Only one full dynamical calculation is needed for each reference structure, so that the use of the TLEED approximation as the basis of the automated structure search results in large computational savings.

However, it should be noted that this 'divide and conquer' approach simply converts one NP complete problem to another, since the number of reference structures from which local searches must be launched still scales exponentially with the number of parameters varied. In practice, this does not appear to be a serious difficulty since descent methods have been quite successful empirically in locating the best-fit structure in actual LEED crystallographic studies using only a few reference structures [10]. The physical reason for the apparent success of descent methods can been seen in figure 8, which shows the distribution of $R$-factor values at the extrema of local minima of the Ir(110)-p(2 × 1) surface. This distribution was calculated from exhaustive searches of 1 Å$^3$ of the Pendry $R$-factor hypersurface. We see that the majority ($\simeq$ 90%) of the local minima have $R$-factor values that are normally distributed about the mean. A fit to a Gaussian curve is shown by the full curve in this figure, which indicates that a deviation from the normal distribution occurs only for a small proportion of the minima ($\simeq$ 2%) that have $R$-factor values considerably smaller than the mean.

The form of this distribution indicates that the normally distributed local minima arise from random fluctuations of Pendry $R$-factor as the structural parameters are varied. The statistical origin of this topographic feature is anticipated by the work of Pendry [46]. This

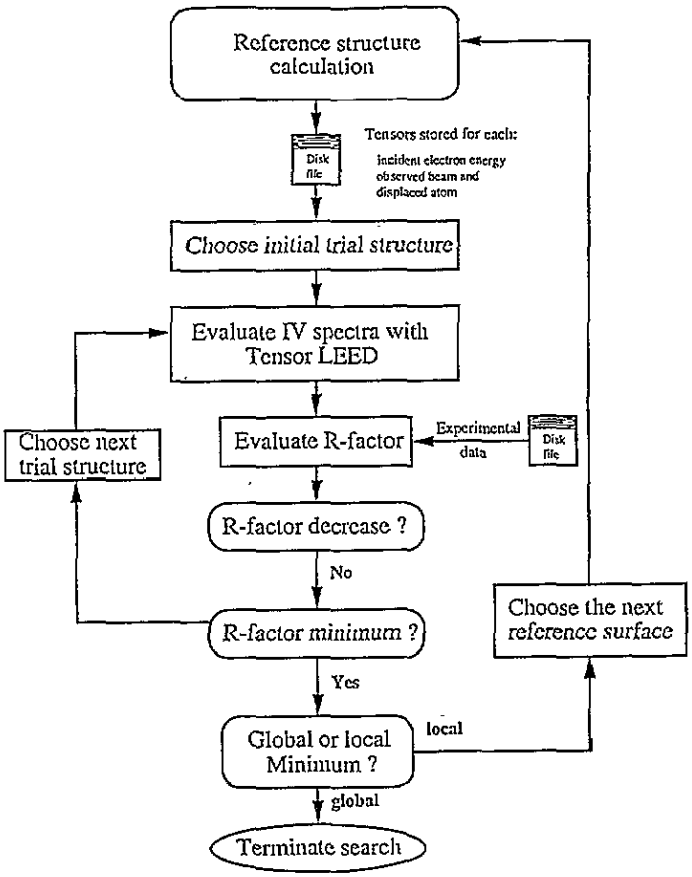


**Figure 7.** A flowchart for $R$-factor optimization by TLEED. The reference structure calculation is a self-contained program that generates the tensors $T$ for the best guess structure. The remainder of the calculation is performed by a single program that combines the calculation of $IV$ spectra by TLEED and *in situ* $R$-factor optimization.

model predicts that, in a region of parameter space where there is no physical, and only random, correlations between the trial and actual surface structure, the Pendry $R$-factor fluctuates with a standard deviation, $\sigma_R$, from the mean, $\langle R \rangle$, given by

$$\frac{\sigma_R}{\langle R \rangle} \simeq (3V_{0i}/\Delta E)^{1/2}. \tag{5.1}$$

Here $V_{0i}$ is the imaginary part of the potential in the surface (approximately half the peak width in the $IV$ spectra) and $\Delta E$ is the total energy range of the experimental data-set. For the Ir(110) case considered here the predicted ratio of the standard deviation of the Pendry $R$-factor to the mean given by equation (5.1) is 0.15, a value that is in excellent agreement with the results shown in figure 8.

This analysis indicates that the majority of the local minima of the Pendry $R$-factor hypersurface (for the Ir(110)-p(2 × 1) case at least) arise from random fluctuations. Furthermore, these random local minima are shallow and have relatively high $R$-factor values, which lie within (2–3)$\sigma_R$ of the mean ($\langle R \rangle \simeq 0.80$). The minima that deviate from the Gaussian curve on the low-$R_P$ side of the normal distribution have a different physical origin. These minima correspond to the diffraction coincidences [21] and occur because of

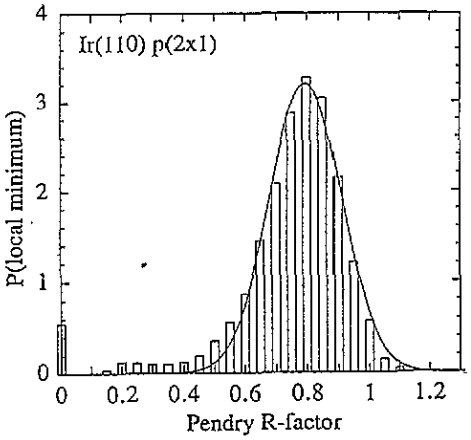


**Figure 8.** A histogram showing the distribution of $R$-factor values at local minima of the Ir(110) p(2 × 1) Pendry $R$-factor hypersurface. The full curve is a least-squares fit of the peak to a normal distribution with $\langle R \rangle = 0.80$ and $\sigma_R = 0.12$.

the periodic satisfaction of the Bragg condition as each atom is displaced through half of the electron wavelength. Thus, the overall topography of the Pendry hypersurface may be described as having a few smooth deep valleys between relatively rough 'highland' regions. This result explains, in part, the success of local searches, which always proceed downhill from the launch point in parameter space. If a local search is launched from a point in parameter space that has an $R$-factor significantly below the mean (uncorrelated) value, then the majority of $R$-factor minima are avoided and most of the minima encountered are either the global minimum or diffraction coincidences. Nevertheless, in principle, the intrinsic difficulties associated with local search algorithms can be overcome with a global optimization method for LEED [47] such as simulated annealing [48–51].

Compared to exhaustive surveys, the automated (local) descent methods with TLEED greatly improve the scaling of the search effort with the number of parameters varied. An estimate of the scaling relation for descent methods can be obtained by noting that the location of the minimum of a single quadratic basin requires the evaluation of $IV$ spectra from a number of trial structures that scales as $M(M+1)$. Such scaling appears to be realized approximately in actual LEED structure searches using gradient methods [10], which are found to scale as $M^2$. In addition, the TLEED calculations of the $IV$ spectra for each trial structure scale linearly with the number of displaced atoms. Since the number of structural parameters is often proportional to the number of displaced atoms (e.g. the position of $N$ atoms is given by $M = 3N$ coordinates), then the overall scaling of ATLEED is approximately cubic in the number of determined structural parameters. This is to be compared with an exhaustive search using full dynamical calculations that scales as $N^3C^M$.

An estimate of the scaling relation for a global search method, the simulated annealing (SA) algorithm has been obtained for the Ir(110)-p(2 × 1) system in which four to six parameters were varied. The parameters included in the theory–theory comparison were the first three interlayer spacings and the row pairing and buckling of the top three Ir atomic planes parallel to the missing rows. For $M = 4$, $M = 5$ and $M = 6$, the total volume of parameter space explored was 1 Å$^4$, 1 Å$^5$ and 1 Å$^6$, respectively. The number of local minima discovered by an exhaustive search of these parameter spaces was 102 for $M = 4$ and 397 for $M = 5$. An exhaustive search of the six-dimensional $R$-factor hypersurface would have required the calculation of $IV$ spectra from approximately $10^6$ structures and

was not computationally feasible with any machines currently available to us. We note that the density of minima appears to scale approximately as $C^M$, which would be expected from simple geometrical arguments.

The number of trial structures required for the SA search versus the number of structural parameters is shown as a log–log plot in figure 9. The good fit to a straight line indicates that the scaling relation is polynomial in the number of varied parameters. Least squares fitting determined the exponent to be $M = 6.0 \pm 0.3$. For comparison, also shown in figure 9 is the non-polynomial scaling curve for an exhaustive search (which depends exponentially upon the number of varied parameters). We note that the simulated annealing algorithm has a much less favourable scaling relation than a single local search. However, the existence of local minima means that the local search must be repeated a number of times that scales exponentially with the number of varied parameters. For sufficiently complex surfaces, simulated annealing may be more efficient than multiple launch local searches.

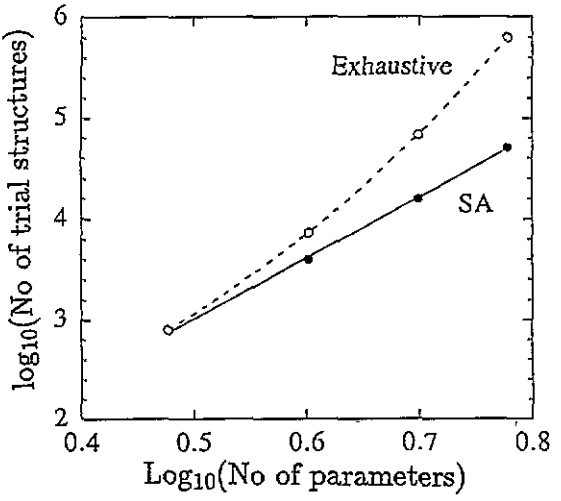


**Figure 9.** A log–log plot of the average number of trial structures investigated by a search algorithm as a function of the number of structural parameters. The scaling relation of the simulated annealing algorithm (•) fits to a straight line that has slope $6.0 \pm 0.3$. For comparison the exponential scaling behaviour of an exhaustive search is shown (○).

## 6. Applications of TLEED theory: structure determination

Table 1 shows the thirty-two unknown surface structures that have been solved and published by TLEED up to mid-1994. The bulk of these surface structures have been investigated using automated search algorithms in combination with TLEED (ATLEED).

## 7. New structural methods based upon tensor LEED concepts

### *7.1. Introduction*

In this section, we review some of the extensions and applications of TLEED theory to LEED analysis. The central concept of TLEED theory is that distortions of a reference surface may be treated perturbatively and that this treatment leads to great increases in computational efficiency. These distortions are not confined to structural displacements; for example, the

**Table 1.** Tabulation of surface structures solved by the TLEED technique. The majority of the listed structures were solved by TLEED combined with an automated search algorithm (ATLEED).

| System | Method | Reference |
|---|---|---|
| W(1 0 0)-O (disordered) | TLEED | [11] |
| Mo(1 0 0)-c(2 × 2)-S | ATLEED | [78, 79] |
| Mo(1 0 0)-c(2 × 2)-C | ATLEED | [79] |
| Rh(1 1 1)-(2 × 2)-$C_2H_3$ | ATLEED | [80] |
| Pt(1 1 1)-(2 × 2)-$C_2H_3$ | ATLEED | [81] |
| Pt(1 1 1) | ATLEED | [82] |
| Pt(1 1 1)-(2 × 2)-O | ATLEED | [82] |
| Re(0 0 0 1)-(2 × 2)-S | ATLEED | [83] |
| Re(0 0 0 1)-(2$\sqrt{3}$ × 2$\sqrt{3}$)R30$^0$-S | ATLEED | [83] |
| $\beta$-SiC(1 0 0)-c(2 × 2) | ATLEED | [84] |
| $\beta$-SiC(1 0 0)-p(2 × 1) | ATLEED | [85] |
| $Mo_xRe_{1-x}$(1 0 0) | ATLEED | [65] |
| Cu(110)-(2 × 3)-N | ATLEED | [86] |
| Ni(1 1 1)-p(2 × 2)-$CH_3CN$ | ATLEED | [87] |
| Si(1 0 0)-(2 × 2)-Al | ATLEED | [88] |
| $Pt_3Ti$(1 1 1) | ATLEED | [89] |
| Rh(1 1 1) ($\sqrt{3}$ × $\sqrt{3}$)-I | ATLEED | [90] |
| Ni(1 1 1)-c(4 × 2)-2NO | ATLEED | [91, 92] |
| Pt(1 1 1)-p(2 × 2)-NO | ATLEED | [92] |
| Rh(110)-p2mg(2 × 1)-2CO | ATLEED | [93] |
| Rh(1 1 1)-($\sqrt{3}$x$\sqrt{3}$)-2CO | ATLEED | [94] |
| Pt(1 1 1)-$C_6H_6$-CO | ATLEED | [95] |
| Rh(1 1 1)-$C_6H_6$-CO | ATLEED | [95] |
| $Fe_3O_4$(1 1 1) | ATLEED | [96] |
| Pt(1 1 1)-$Fe_3O_4$ (multilayer) | ATLEED | [97] |
| $H_2O$(0 0 0 1) (ice) | ATLEED | [98] |
| W(1 0 0)-Cu | ATLEED | [99] |
| Si(1 0 0)-(2 × 1)-Cs | ATLEED | [100] |
| Si(1 0 0)-(2 × 1)-K | ATLEED | [100] |
| Rh(1 0 0)-c(2 × 2)-S | ATLEED | [101] |
| Rh(1 0 0)-p(2 × 2)-S | ATLEED | [101] |

chemical replacement of one atom in the reference surface with another may be treated by a variation of TLEED theory. In addition, the success of the TLEED approximation has led to the development of novel approximation schemes that exploit similar physical approximations to full multiple scattering, such as linear LEED.

### *7.2. Linear LEED*

Linear LEED (LLEED) is a new approximate method that has been developed to perform coarse surveys of structural parameter space [52]. Since LLEED is designed to explore larger areas of the structural parameter space than TLEED, it is particularly useful when used in conjunction with TLEED. LLEED allows the exploration of combinations of atomic displacements involving the simultaneous displacement of several atoms in the reference structure. It is assumed that these displacements make linearly independent contributions to the scattered amplitude. This assumption, when valid, leads to significant computational savings compared to full dynamical calculations.

Consider a surface structure in which we wish to locate one structural coordinate of $N$ atoms. Therefore we are performing a search for $N$ structural parameters within an $N$-

dimensional hypercube of parameter space. In LLEED, just as in TLEED, full dynamical LEED calculations are performed for reference structures. However, in contrast to TLEED, for LLEED full dynamical calculations are performed for several reference structures, which correspond to points in parameter space that lie along the edges of the hypercube (see figure 10).

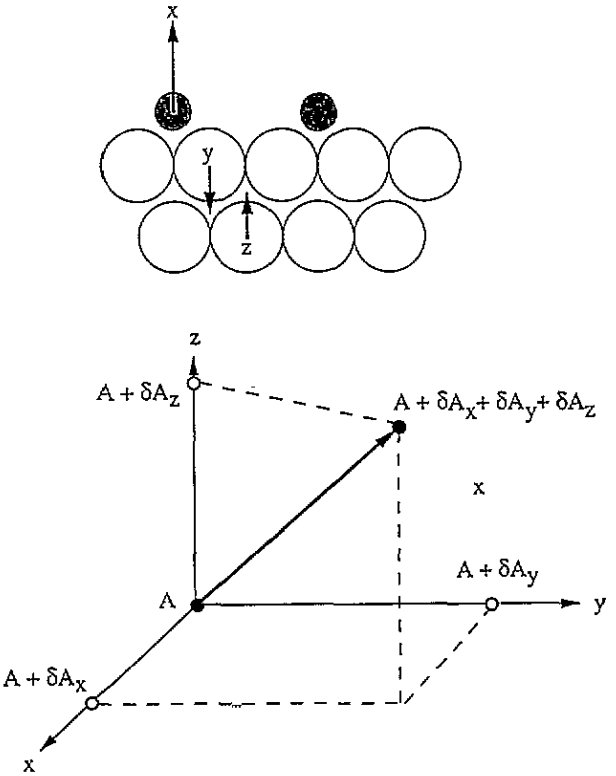


**Figure 10.** A schematic illustration of the linear LEED approximation. Shown is a three-dimensional hypercube corresponding to the parameter space of three structural parameters. The surface structure corresponding to any combination of these three parameters is a point somewhere inside the cube. In the linear LEED approximation, full dynamical calculations are performed to compute the change in the LEED amplitudes for structures corresponding to points along the edge of the hypercube. The reference structure, with respect to which these changes are measured, is one corner of the hypercube. The change in amplitude for any point in parameter space inside the cube is considered to be the superposition of the changes in amplitude calculated at the projected points on the edge of the hypercube. This is an approximation if the structural parameters are correlated.

In LLEED, it is assumed that the LEED amplitude for a surface represented by a point in parameter space inside the cube is simply a linear combination of the LEED amplitudes for the corresponding points of the edge of the hypercube. Since simply adding together a set of amplitudes has virtually no computational overhead, the time taken to explore the entire hypercube is dominated by the reference structure calculations. Since the number of reference structure calculations scales linearly with the number of structural parameters, the time taken to explore the region of parameter within the hypercube scales linearly with $N$ rather than exponentially. Not only is this scaling more advantageous than a directed search but, if the LLEED approximation is valid, LLEED can be used to exhaustively search

the parameter space. Consequently, the problem of distinguishing between global and local minima does not arise.

In the LLEED approximation, it is assumed that variations in the structural parameters make linearly independent contributions to the scattered amplitude. This precludes the use of the approximation to consider different coordinates of the same atom as independent structural parameters. This circumstance requires one reference calculation for every possible position of the atom and destroys the linear scaling of the method. Further, linear independence requires that there is no correlation in the scattered amplitude between variations of any pair of structural parameters. This approximation is exact in the kinematic limit where the scattered amplitudes from each atom are summed to obtain the total scattered amplitude, but, in the presence of multiple scattering, LLEED is an approximation. Multiple scattering allows electrons to follow paths that link together a pair of atoms. Consequently, multiple scattering causes correlations between two displaced atoms to be present in the LEED amplitude. Just as in our discussion of TLEED, these correlated multiple scattering paths can be classified into two types: those on which an electron returns to the same (displaced) atom more than once, and those on which the electron scatters between two or more different displaced atoms. In contrast to TLEED, LLEED treats the closed multiple scattering paths exactly since a full dynamical calculation is performed for each independent displacement of an atom. Both TLEED and LLEED completely neglect open multiple scattering paths that link together displaced atoms.

In our discussion of sections 3.3 and 3.4, we have argued that multiple scattering correlations limit the radius of convergence of the TLEED approximation. Further we have argued that the open scattering paths are the most important source of correlations in LEED $IV$ spectra. Thus it would appear, in principle, that the LLEED approximation would have the same radius of convergence as TLEED. In the initial applications of the method, this is found not to be the case [41]. This suggests that LLEED can be a good approximation in cases where scattering between displaced atoms is unimportant. An obvious case is a surface where the displaced atoms are further apart than the inelastic scattering length of the electrons. In this case the LLEED approximation is an excellent model of a full dynamical calculation whatever the magnitude of the atomic displacements. By comparison, TLEED will always suffer from finite radius of convergence in this case since, in contrast to LLEED, it neglects the closed multiple scattering paths that become important as the atomic displacements grow.

### *7.3. Direct methods*

Pendry *et al* have proposed a direct method for LEED, based upon TLEED theory [30, 53–56]. Instead of attempting an inversion of a set of $IV$ spectra, one considers the difference between the measured $IV$ spectra and those calculated for a reference surface. The direct method then extracts the atomic positions from this difference spectrum. The fundamental advantage of this approach is that the difference spectrum can be interpreted perturbatively by TLEED theory and avoids the use of a full dynamical calculation. This approach is related, at least conceptually, to the holographic techniques recently proposed for the interpretation of electron scattering at surfaces [57–59]. If we regard the amplitude scattered from the reference surface as a reference wave, the intensity spectra from a trial surface are produced by the interference of this wave with an object wave that is scattered by the perturbation produced by the atomic displacements [60, 61].

Pendry *et al* have used this approach to the determination of the interlayer spacings and adsorption heights for several simple systems: Rh(110), Rh(110)-(1 × 1)-2H, W(1 0 0) [30], Ni(1 0 0)-c(2 × 2)-O [55, 56], Ni(1 0 0)-p(2 × 2)-O [56] and Ni(1 0 0)-c(2 × 2)-S [56].

In each of these cases the reference structure was the bulk termination of the solid and the displacements directly determined were 0.1 Å or less. The magnitude of the retrieved displacements is limited because this version of the direct method employs the linear version of TLEED theory which fails for larger displacements. A more sophisticated scheme, based on the full TLEED theory, has been proposed and applied to one test case [62]. In principle, this development should enable the application of the direct method to surfaces in which the actual atomic positions deviate by more than 0.2 Å from their positions in the reference structure.

Despite this development, the direct methodology has a number of disadvantages compared to more conventional methods. First, it requires the comparison of absolute experimental and theoretical intensities, a generally undesirable procedure since it is well known that static and dynamic disorder within the surface usually leads to significant disagreement between the absolute intensity of calculated and experimental $IV$ spectra. While this deficiency can be overcome by using $R$-factor methods, this would add significantly to the complexity of the method and the inversion procedure. In addition, the direct method requires the solution of an overdetermined set of simultaneous equations, which relate the intensity differences to the atomic displacements (typically there are many times more experimental energy points than structural parameters to be determined). This represents a difficult and unstable numerical problem, which has no exact solution. Its solution requires sophisticated and time-consuming computational techniques.

A principal advantage of these direct methods is that they avoid the problem of local versus global minima. Thus, although the initial results of this approach appear promising [63], the direct method requires further development before it can be considered as a reliable alternative to trial-and-error or optimization methods.

### *7.4. Chemical TLEED*

*7.4.1. Introduction* The Erlangen group has applied the TLEED formalism to the treatment of chemical displacements; the substitution of one surface atom (such as O) for another (such as S) [64–66]. This distortion of the surface composition is described by a change of the atomic $t$-matrix for the substituted atom. For instance, if atom A is replaced by atom B then

$$\delta t = t_B - t_A. \tag{7.1}$$

The TLEED method can be used to treat chemical substitution by performing the reference structure calculation for a surface with a particular chemical composition. Then the $IV$ spectrum from a trial structure with a different chemical composition is computed by the TLEED approximation with $\delta t$ given by equation (7.1).

In order for the TLEED approximation to be valid in the case of chemical substitution, the change in the $t$-matrix must be small compared to the $t$-matrix of either atomic species. This implies that the scattering factors of atoms A and B must, in some sense, be similar. Therefore, a necessary condition for the application of chemical TLEED is that the difference between the total scattering cross section of the atom pair is small compared to the scattering cross section of either atom.

*7.4.2. Chemical substitution in overlayer systems* The Erlangen group have tested the chemical TLEED approximation in three cases [64]. First, a reference calculation was performed for a Ni(1 0 0)-(1 × 1)-O overlayer system in which the oxygen adatoms were placed $d = 1$ Å above the hollow adsorption site. The chemical TLEED approximation was then used to calculate $IV$ spectra from a trial structure in which every second oxygen atom

was replaced with a vacancy, thus creating a Ni(1 0 0)-c(2 × 2)-O overlayer. The results of this trial structure calculation were then compared to a full dynamical calculation for the Ni(1 0 0)-c(2 × 2)-0 surface using the Pendry $R$-factor (see figure 11). The $R$-factor between the chemical TLEED and full dynamical calculations was found to be $R_P = 0.19$, a value that is similar to the level of agreement obtained between full-dynamical theory and experiment for this type of overlayer system.

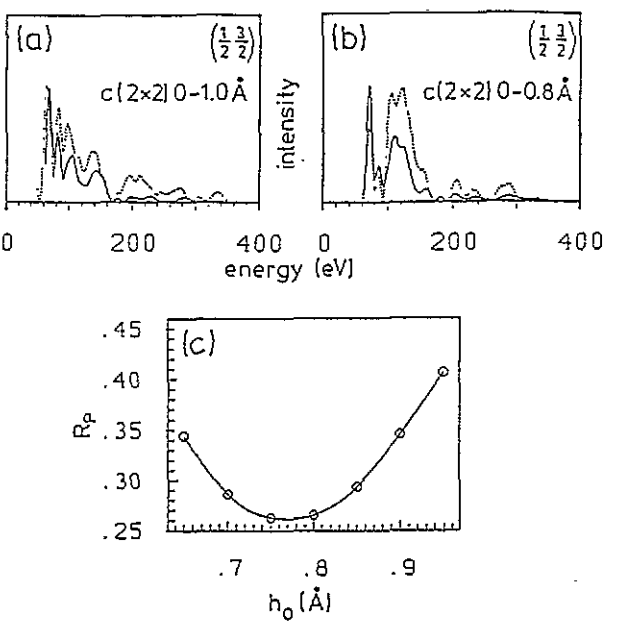


**Figure 11.** Comparison of the LEED $IV$ spectra of a fractional-order beam of the Ni(1 0 0)-c(2 × 2)-O surface computed using a full dynamical (FD) calculation (full curves) and by chemical TLEED (dashed lines). The reference structure for the chemical TLEED calculation was a Ni(1 0 0)-(1 × 1)-O surface with an adsorption height of $h = 1.0$ Å. (*a*) Comparison for $h = 1.0$ Å. (*b*) Comparison for $h = 0.8$ Å. In this case chemical TLEED is combined with (geometrical) TLEED to perform both chemical substitution and the relaxation of the overlayer spacing. (*c*) The $R$-factor comparing the FD calculation at $h = 0.8$ Å and the combined chemical TLEED/TLEED calculation for the Ni(1 0 0)-(1 × 1)-O reference surface where $h = 1.0$ Å. (After Doll *et al* [64]).

These results suggest that multiple scattering between the oxygen atoms in the (1 × 1) overlayer makes a significant contribution to the $IV$ spectra from this overlayer system. If there was no multiple scattering among atoms in the overlayer, then the chemical TLEED approximation would be exact. Consequently the $R$-factor value of 0.19 represents, at least approximately, the effect upon the $IV$ spectra of neglecting multiple scattering between the O atoms. Despite this relatively large $R$-factor value, the authors were able to show that the O adsorption height of $d = 0.77$ Å could be determined within 0.03 Å by combining chemical tensor LEED with the conventional (geometrical) TLEED approximation and starting with the reference structure described above. This suggests that chemical and geometrical displacements are only weakly correlated in the $IV$ spectra and that there is no structural information loss associated with the adoption of the chemical TLEED approximation.

A less radical perturbation of the reference structure, where the chemical TLEED approximation should work much better, is the replacement of the oxygen atoms with sulfur atoms. The Erlangen group have tested this idea by performing a reference structure

calculation for Ni(1 0 0)-p(2 × 2)-O and then used chemical TLEED to chemically substitute S atoms for O to create a Ni(1 0 0)-p(2 × 2)-S trial structure (figure 12). In this case the level of agreement between the chemical TLEED calculation and a full dynamical calculation for Ni(1 0 0)-p(2 × 2)-S is of the order of $R_P \simeq 0.05$. Thus chemical TLEED is successful, *despite the strong disagreement between the IV spectra for Ni(1 0 0)-p(2×2)-S and Ni(1 0 0)-*p(2×2)-O; $R_P = 0.78$. This suggests that multiple scattering among the adatoms is relatively unimportant for this dilute overlayer system, so that the scattered amplitude is dominated by multiple scattering paths on which the electrons scatter from an adatom only once. Whilst, in comparison to a (1 × 1) overlayer, one anticipates that the (open) multiple scattering paths linking different adatoms are relatively unimportant in determining the *IV* spectra for such an open (p(2 × 2)) overlayer, closed paths, on which an electron returns to the same adatom via backscattering from the substrate, are not suppressed. This suggests that such closed paths do not make a significant contribution to the scattered intensity, independent of the density of adatoms in the overlayer. This is in agreement with our discussion of the failure of TLEED given in sections 3.3 and 3.5.

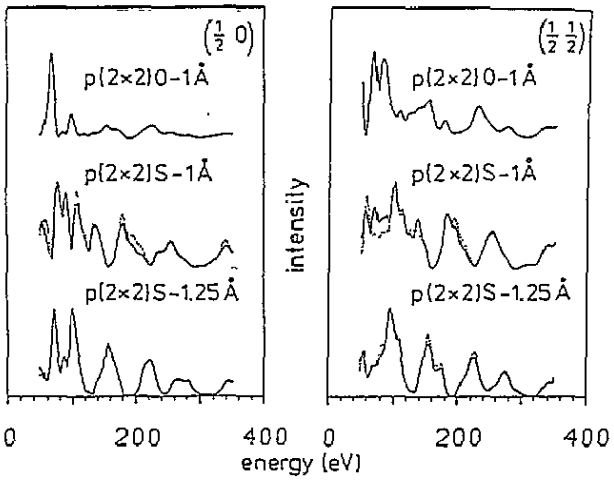


**Figure 12.** Comparison of the LEED *IV* spectra of two fractional-order beams of Ni(1 0 0)-p(2×2)-S. Dashed lines: spectra computed by chemical TLEED starting with a Ni(1 0 0)-p(2×2)-O reference structure. Solid lines: full dynamical calculation. (After Loffler *et al* [69]).

*7.4.3. Disordered alloy surfaces* An important application of chemical TLEED is to the surface structure and compositional determination of disordered alloy surfaces [64, 65]. To date, LEED studies of random alloys have relied universally upon the comparison of experimental *IV* spectra with the results of theoretical calculations that employ the average *t*-matrix approximation (ATA) to simulate the effects of substitutional disorder [67]. Empirical support for the validity of this approximation is to be found in the agreement between the LEED results for $Ni_xPt_{1-x}$ and those from both atomistic studies and other composition sensitive experimental techniques [67]. More recently the validity of ATA was confirmed by *comparison with the coherent-potential approximation method* (CPA) [40]

The underlying difficulty encountered when one attempts the calculation of LEED *IV* spectra from random alloys is the lack of periodicity parallel to the surface, which is a consequence of the substitutional disorder. The usual approach is to employ the ATA approximation [67], so that the disorder is incorporated indirectly and the actual alloy is modelled by an ordered surface in which the atomic scattering is described by an effective

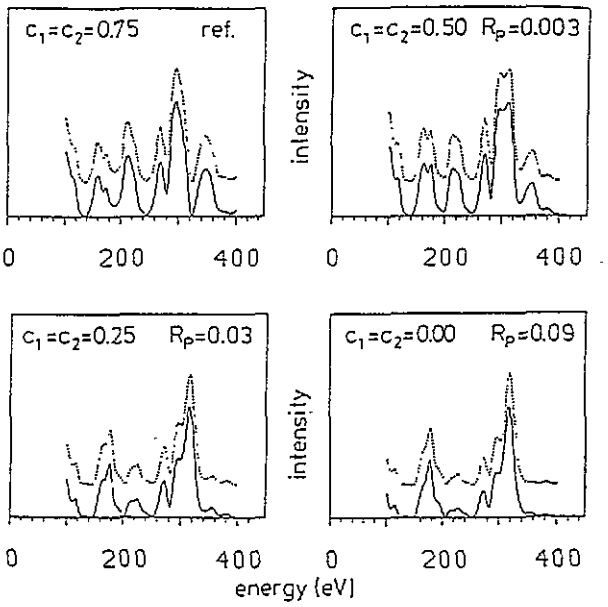


**Figure 13.** Comparison of the LEED $IV$ spectrum of the [1 0] beam of the $Mo_{75}Re_{25}$ disordered alloy surface computed using a full dynamical ATA-LEED calculation (full curves) and using chemical TLEED (dashed lines). The curves are compared by the Pendry $R$-factor $R_P$. (After Doll *et al* [64]).

$t$-matrix calculated by a simple compositional average of the $t$-matrices of the individual alloy components. If we restrict our attention to a binary alloy comprising atom types A and B and recognize that close to the surface the composition may be layer dependent, this effective $t$-matrix is given by

$$t^I_{ata} = c_I t_A + (1 - c_I) t_B. \tag{7.2}$$

Here $c_I$ is the concentration of species A in layer $I$ and $t_A$ is the usual atomic $t$-matrix for atom type A. Unfortunately, the average $t$-matrix is an input to the full dynamical calculation. Consequently, in order to fit the surface layer compositions to the experimental spectra, it is necessary to repeat full dynamical calculations for every 'trial' surface segregation profile.

To apply TLEED to this case we perform the reference structure for a surface with a particular set of layer compositions which are as close as possible to the true layer compositions. If the composition is changed by an amount $\delta c_I$ then the corresponding change in the $t$-matrix is

$$\delta t = \delta c_I (t_A - t_B). \tag{7.3}$$

The calculation of the change in the scattered amplitude and the $IV$ spectra of the trial structure then proceed using the usual TLEED formalism.

One expects that the compositional radius of convergence of the chemical TLEED technique is strongly dependent upon the difference between the scattering properties of the two components of the alloy. If the atomic $t$-matrices of the atoms are similar, then change in the composition can be large. Conversely, if the atoms are dissimilar, then the compositional radius of convergence will shrink.

*7.5. Thermal tensor LEED*

This method has been tested by calculating the $IV$ spectra of a $Mo_{75}Re_{25}(1\,0\,0)$ surface using chemical tensor LEED and fully dynamical calculations using the ATA method (figure 13). The reference structure calculation was performed for the bulk termination of the alloy so that $c_I = 0.75$ in all atomic layers parallel to the surface. From figure 13 it is clear that the chemical tensor LEED method agrees well with the results of the full dynamical calculation over the entire range of possible Mo concentrations in the first two atomic planes. In no case is the Pendry $R$-factor between the chemical TLEED and fully dynamic (ATA-LEED) calculations greater than 0.1. This agreement is quite remarkable since Mo ($Z = 42$) and Re ($Z = 75$) lie quite far apart in the periodic table and therefore should have dissimilar scattering factors. It remains to be seen if this promising method can be applied to systems such as NiPt where the atomic scattering of each component is even more dissimilar.

Tensor LEED is ideally suited for the treatment of small displacements of surface atoms from their equilibrium positions. Just this circumstance arises when one considers thermal vibrations of surface atoms [68]. Recently, the Erlangen group has adapted TLEED to treat the influence of isotropic thermal vibrations of surface atoms upon LEED $IV$ spectra [69]. The resulting method is called thermal TLEED.

In a fully dynamical LEED calculation the effect of isotropic thermal vibrations upon the electron scattering is incorporated by computing a set of complex, temperature dependent phase shifts. In particular, the atomic $t$-matrix of an atom vibrating with mean-squared amplitude $\langle \delta r^2 \rangle$ is given by [69]

$$t_\ell(T, \theta_D) = \sum_{\ell} \sum_{\ell'} i^{\ell''} \left[4\pi(2\ell''+1)(2\ell'+1)(2\ell+1)\right]^{1/2} \times \exp\left[-\frac{1}{3}\langle \delta r^2 \rangle (T) \kappa^2\right] j_{\ell'}\left[-i\frac{1}{3}\langle \delta r^2 \rangle (T)\right] C_{\ell 0, \ell' 0, \ell'' 0} \tag{7.4}$$

where $C$ is a Gaunt coefficient. The mean-squared amplitude $\langle \delta r^2 \rangle$ is related to the Debye temperature through

$$\left(\langle \delta r^2 \rangle_T\right) \simeq (9\hbar/4mk\theta_D)\left(1 + (16T^2/\theta_D^2)\right)^{1/2} \tag{7.5}$$

Unfortunately, the phase shifts are an input to a full dynamical calculation. Consequently, in order to fit the surface Debye temperature to the experimental spectra, it is necessary to repeat full dynamical calculations for every 'trial' Debye temperature.

The fundamental idea of thermal TLEED is to describe the thermal vibrations perturbatively using TLEED theory to treat the dynamic thermal atomic displacements. The reference structure calculation is performed at finite temperature using a particular set of 'reference' Debye temperatures, usually chosen to be as close as possible to the actual Debye temperatures of each surface atom. In the reference structure calculation, the complex temperature-dependent atomic $t$-matrix of each of the surface atoms is calculated from the vibrational amplitudes corresponding to the reference Debye temperatures, equation (7.4). We now consider a trial surface, in which the surface atoms have Debye temperatures that differ from their values in the reference structure, $\theta_D + \delta\theta_D$. The corresponding change in the temperature dependent $t$-matrix is

$$\delta t = t(T, \theta_D) - t(T, \theta_D + \delta\theta_D). \tag{7.6}$$

It is apparent that the $IV$ spectra for the trial surface may be evaluated by the usual TLEED formalism, using this $\delta t$ in place of the usual geometrical change in the $t$-matrix.

Since most thermal vibrational amplitudes are smaller that 0.2 Å, our experience with TLEED leads us to expect that thermal TLEED will reproduce the results of the corresponding

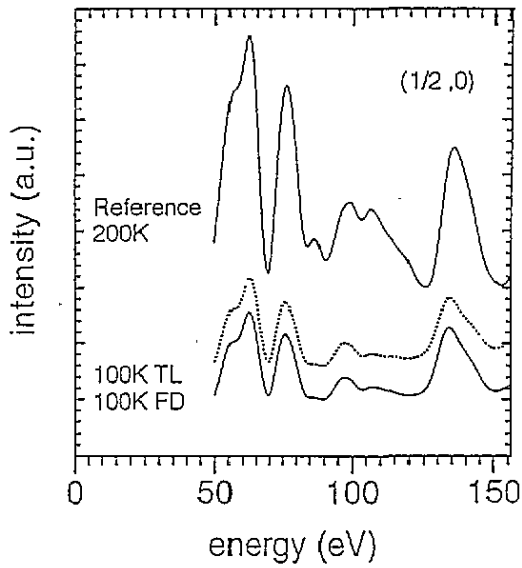


**Figure 14.** Comparison of the LEED *IV* spectra of the (1/2,0) beam of Ni(1 0 0)-c(4 × 2)-K calculated using TTLEED and a FD calculation for a potassium Debye temperature of 200 K and 100 K. Full curves: full dynamical calculation using complex phase shifts. Dashed line: thermal TLEED calculation for $\theta_D = 100$ K starting with a reference structure where $\theta_D = 200$ K. (After Loffler *et al* [69]).

full-dynamical LEED calculation. This is found to be the case in practical applications of the method. Loffler *et al* [69] have tested thermal TLEED when it is applied to a variety of systems. An example of the level of agreement between thermal tensor LEED and a full-dynamical calculation using complex phase shifts is shown in figure 14, which displays the *IV* spectrum of the (1/2,0) beam for Ni(1 0 0)-c(4 × 2)-K calculated by both methods.

In addition, experimental *IV* spectra for Ni(1 0 0) taken at 100K were used to determine the surface Debye temperatures for the first two atomic layers. The reference structure calculation employed the bulk Debye temperature of 440 K for atoms in every atomic plane. Application of thermal TLEED led to values of $\theta_D = 250 \pm 50$ K in the first layer and $\theta_D = 350 \pm 100$ K in good agreement with the average Debye temperature of 335 K determined by a fully dynamical calculation in which the Debye temperature of all atoms was identical. Similar level of agreement is when thermal tensor LEED is applied to Ni(1 0 0)-c(4 × 2)K. It is interesting to note that the root-mean-squared amplitude of the Ni atom in the top Ni layer ($\theta_D = 250 \pm 50$ K) is 0.21 Å compared to the amplitude in the reference structure ($\theta_D = 440$ K), 0.13 Å. Clearly, the difference in the mean displacement is smaller than 0.15 Å, well within the radius of convergence of TLEED.

Döll *et al* have also demonstrated that the thermal and geometric displacements are almost uncorrelated. This shows that the thermal and structural parameters may be fitted simultaneously by TLEED and thermal tensor LEED. Finally we note that thermal TLEED is easily generalized to anisotropic vibrations of surface atoms, which would be simply described by a non-diagonal change in the *t*-matrix.

### *7.6. Future applications of TLEED*

The perturbative approach that forms the foundation of the TLEED approximation may be applied to other electron-based techniques for surface structure determination such as

photoelectron diffraction (PED) [70], Auger electron diffraction (AED) [70], high-resolution electron energy loss spectroscopy (HREELS) [71] and near-edge x-ray absorption fine structure (NEXAFS) [72]. Structure determination using any of these methods requires an adequate computational model of multiple scattering. Since the electron energies involved are similar to those employed for LEED it is likely that the radius of convergence of any adaptation of the TLEED approach will be sufficient to reduce greatly the amount of computational effort required for the structure determination using these techniques. The TLEED formalism combined with an automated search algorithm has been applied recently to photoelectron diffraction [73] and high-energy electron diffraction [74, 75]. The linear LEED method, adapted from the TLEED technique, has also been applied to photoelectron diffraction [76, 77].

## Acknowledgments

The TLEED technique has been developed over a period of almost a decade and still continues to be improved, applied to new systems and used as the basis of new approaches to surface crystallography. In this section I would like to acknowledge the many individual researchers and groups that have made important contributions to the technique.

In the spring of 1985, the original idea for TLEED was suggested to the author as a PhD research project by John Pendry FRS at Imperial College, London. During this period, we benefited greatly from discussions with Professor Klaus Heinz and Norbert Bickel. The London–Erlangen collaboration led by John Pendry and Klaus Heinz has since produced several novel applications of TLEED that are described in this review, in particular the development of direct methods based on TLEED and chemical and thermal TLEED.

The first version of the TLEED codes was developed by the author and published in 1989 as part of the CPC library [14, 15]. During 1988–89 the author worked with Michel Van Hove on further developments of the TLEED method that expanded the theory to treat many atoms in the surface unit cell and combined an automated search algorithm with the TLEED [45] (ATLEED). In addition to the Berkeley ATLEED codes, the original set of published programs have also been developed, independently, by the Imperial, Erlangen and York groups. The York group, led by S P Tear, has combined TLEED with their own suite of optimization algorithms.

Since 1990, the Berkeley group of Adrian Wander, Nick Materer, A Barbieri and M A Van Hove generalized the ATLEED codes to more complex reference structures and made significant improvements in both the reliability and the efficiency of the optimization algorithm used for automated searching. This group has proceeded to use the method to solve several unknown surface structures. Some of these surface structures represent the most complex surface structures solved to date by LEED. The ATLEED codes are now available as part of the Berkeley LEED tape maintained by M A Van Hove, from whom copies of the programs may be obtained.

## References

[1] Somorjai G A 1981 *Chemistry in Two Dimensions: Surfaces* (Ithaca, NY: Cornell University Press)
[2] Zangwill A 1987 *Physics at Surfaces* (Cambridge: Cambridge University Press)
[3] Duke C B 1994 *Surface Science: The First Thirty Years* (Amsterdam: North-Holland)
[4] Pendry J B 1994 *Surf. Sci.* **299/300** 375
[5] Tong S Y 1994 *Surf. Sci.* **299/300** 358
[6] Marcus P M 1994 *Surf. Sci.* **299/300** 447

*Watson P R, Van Hove M A and Hermann K 1993 NIST Surface Structure Database Ver. 1* (Gaithersburg, MD: National Institute of Standards and Technology)
[8] Heinz K 1994 *Surf. Sci.* **299/300** 447
[9] Rous P J 1994 *Prog. Surf. Sci.* **39** 3
[10] Van Hove M A, Moritz W, Over H, Rous P J, Wander A, Barbieri A, Materer N, Starke U and Somorjai G A 1992 *Tutorials on Selected Topics In Modern Surface Science* (Amsterdam: Elsevier)
[11] Rous P J, Pendry J B, Saldin D K, Heinz K, Müller K and Bickel N 1986 *Phys. Rev. Lett.* **57** 2951
[12] Rous P J and Pendry J B 1989 *Surf. Sci.* **219** 355
[13] Rous P J and Pendry J B 1989 *Surf. Sci.* **219** 373
[14] Rous P J and Pendry J B 1989 *Comput. Phys. Commun.* **54** 137
[15] Rous P J and Pendry J B 1989 *Comput. Phys. Commun.* **54** 157
[16] Heinz K and Müller K *1982 Structural Studies of Surfaces* (Berlin: Springer)
[17] Van Hove M A 1988 *The Chemistry and Physics of Solid Surfaces VII* ed R Vanselow and R F How (Berlin: Springer)
[18] Heinz K 1988 *Prog. Surf. Sci.* **27** 239
[19] Maclaren J M, Pendry J B, Rous P J, Saldin D K, Somorjai G A, Van Hove M A and Vvedensky D D 1987 *Surface Crystallographic Information Service. A Handbook of Surface Structures* (Dordrecht: Reidel)
[20] Van Hove M A and Tong S Y 1979 *Surface Crystallography by LEED* (Berlin: Springer)
[21] Van Hove M A, Weinberg W H and Chan C-M 1986 *Low-Energy Electron Diffraction* (New York: Academic)
[22] Pendry J B 1974 *Low Energy Electron Diffraction* (New York: Academic)
[23] Zimmer R S and Holland B W 1975 *J. Phys. C: Solid State Phys.* **8** 2395
[24] Tong S Y and Van Hove M A 1977 *Phys. Rev.* B **16** 1459
[25] Aberdam D, Baudoing R and Gaubert C 1975 *Surf. Sci.* **52** 125
[26] Heinz K and Besold G 1983 *Surf. Sci.* **125** 515
[27] *Heinz K, Bickel N, Besold G and Müller K 1985 J. Phys. C: Solid State Phys.* **18** 933
[28] Van Hove M A, Lin R F and Somorjai G A 1983 *Phys. Rev. Lett.* **51** 778
[29] Huang H, Tong S Y, Packard W E and Webb M B 1988 *Phys. Lett. A* **130** 166
[30] Pendry J B, Heinz K and Oed W 1990 *Phys. Rev. Lett.* **61** 2953–6
[31] Duke C B 1994 *Surf. Sci.* **299/300** 24
[32] Wander A, Van Hove M A and Somorjai G A 1991 *Phys. Rev. Lett.* **67** 626
[33] Gaspari G D and Gyorffy B L 1972 *Phys. Rev.* B **28** 801
[34] Aers G C, Pendry J B, Grimley T B and Sebastian K L 1981 *J. Phys. C: Solid State Phys.* **14** 3995
[35] Tong S Y, Li C H and Mills D L 1980 *Phys. Rev. Lett.* **44** 407
[36] Grimley T B and Sebastian K L 1980 *J. Phys. C: Solid State Phys.* **3** 5645
[37] Durham P J, Pendry J B and Hodges C H 1982 *Comput. Phys. Commun.* **24** 193
[38] Rous P J 1986 *PhD Thesis* (University of London)
[39] Bickel N, Heinz K, Landskron H, Rous P J, Pendry J B and Saldin D K 1988 *The Structure of Surfaces II* ed J F van der Veen and M A Van Hove (Berlin: Springer) p 19
[40] Crampin S and Rous P J 1991 *Surf. Sci.* **244** L137
[41] Wander A, Pendry J B and Van Hove M A 1992 *Phys. Rev.* B **46** 9897
[42] Cowell P G, Pratton M and Tear S P 1986 *Surf. Sci.* **177** L915
[43] Kleine G, Moritz W, Adams D L and Ertl G 1989 *Surf. Sci.* **219** L637
[44] Kleine G, Moritz W and Ertl G 1990 *Surf. Sci.* **238** 119
[45] Rous P J, Van Hove M A and Somorjai G A 1990 *Surf. Sci.* **226** 15
[46] Pendry J B 1980 *J. Phys. C: Solid State Phys.* **13** 937
[47] Rous P J 1993 *Surf. Sci.* **296** 358
[48] Kirkpatrick S, Gelatt C D Jr and Vecchi M P 1983 *Surf. Sci.* **220** 671
[49] Cerny V 1985 *J. Opt. Theory Appl.* **45** 41
[50] Laarhoven P J M and Aarts E H L 1987 *Simulated Annealing: Theory and Applications* (Dordrecht: Reidel)
[51] Otten R H J M and van Ginneken L P 1989 *The Annealing Algorithm* (Dordrecht: Kluwer Academic)
[52] Pendry J B 1992 *Tutorials on Selected Topics In Modern Surface Science* (Amsterdam: Elsevier)
[53] Pendry J B and Heinz K 1990 *Surf. Sci.* **238** 137–49
[54] Pendry J B, Heinz K and Oed W 1990 *Vacuum* **41** 340–2
[55] Heinz K, Oed W and Pendry J B 1990 *Phys. Rev. B* **41** 10179
[56] *Heinz K, Oed W and Pendry J B 1991 The Structure of Surfaces III* ed S Y Tong, M A Van H K Takayanagi and X D Xie (Berlin: Springer)
[57] Szoke A 1986 *Short Wavelength Radiation: Generation and Applications* ed D J Attwood and J Boker York: American Institute of Physics)

[58] Barton J J 1988*Phys. Rev.* B **61** 1356
[59] Saldin D K, Harp G R, Chen B L and Tonner B P 1991 *Phys. Rev.* B **44** 2480
[60] Szoke A 1993 *Phys. Rev.* B **47** 14044
[61] Hu P and King D A 1993 *Appl. Surf. Sci.* **70** 396
[62] Oed W, Rous P J and Pendry J B 1992 *Surf. Sci.* **273** 261
[63] Pendry J B 1991 *Phil. Trans. R. Soc.* **334** 539
[64] Doll R, Kottcke M and Heinz K 1993 *Phys. Rev.* B **48** 1973
[65] Doll R, Kottcke M and Heinz K 1994 *Surf. Sci.* **307** 434
[66] Doll R, Kottcke M and Heinz K 1994 *Surf. Sci.* **304** 309
[67] Gauthier Y and Baudoing R 1990 *Low Energy Electron Diffraction From Alloy Surfaces* (Boca Raton, FL: CRC Press)
[68] Over H, Moritz W and Ertl G 1993 *Phys. Rev. Lett.* **70** 315
[69] Loffler U, Doll R and Heinz K 1994 *Surf. Sci.* **301** 346
[70] Fadley C S 1990 *Physica Scripta* **T17** 39
[71] Wu Z Q, Xu M L, Chen Y, Tong S Y, Mohamed M H and Kesmodel L L 1987 *Phys. Rev.* B **36** 9329
[72] Stohr J 1993 *NEXAFS Spectroscopy* (Berlin: Springer)
[73] Kaduwela A P, Fadley C S and Van Hove M A 1994 *Phys. Rev.* B at press
[74] Peng L M and Dudarev S L 1993 *Surf. Sci.* **298** 316
[75] Peng L M and Dudarev S L 1993 *Ultramicroscopy* **52** 312
[76] Kaduwela A P, Van Hove M A and Fadley C S 1994 *Surf. Sci. Lett.* **302** L336
[77] Fritzsche V and Pendry J B 1993 *Phys. Rev.* B **48** 9054
[78] Dunphy J, Sautet Ph, Salmeron M, Jentz D, Barbieri A, Van Hove M A and Somorjai G A (unpublished)
[79] Rous P J, Jentz D, Kelly D G, Hwang R Q, Van Hove M A and Somorjai G A 1991 *The Structure of Surfaces III* ed S Y Tong, M A Van Hove, K Takayanagi and X D Xie (Berlin: Springer)
[80] Wander A, Held G, Hwang R Q, Van Hove M A and Somorjai G A 1991 *Surf. Sci.* **249** 21
[81] Starke U, Materer N, Barbieri A, Van Hove M A and Somorjai G A 1993 *Surf. Sci.* **286** 1
[82] Starke U, Materer N, Doll R, Michl M, Heinz K, Barbieri A, Van Hove M A and Somorjai G A (unpublished)
[83] Jentz D, Held G, Barbieri A, Van Hove M A and Somorjai G A (unpublished)
[84] Powers J M, Wander A, Rous P J, Van Hove M A and Somorjai G A 1991 *Phys. Rev.* B **44** 1159
[85] Powers J M, Wander A, Van Hove M A and Somorjai G A 1992 *Surf. Sci.* **260** L7
[86] Vu D T and Mitchell K A R 1994 *Phys. Rev.* B **49** 11515
[87] Gardin D E, Barbieri A and Batteas J D 1994 *Surf. Sci.* **304** 316
[88] Sakama H, Murakami K and Nishikata K 1993 *Phys. Rev.* B **48** 5278
[89] Chen W, Paul J A K and Barbieri A 1993 *J. Phys. C: Solid State Phys.* **5** 4585
[90] Barnes C J, Wander A and King D A 1993 *Surf. Sci.* **281** 33
[91] Mapledoram L D, Wander A and King D A 1993 *Chem. Phys. Lett.* **208** 409
[92] Materer N, Barbieri A, Gardin D, Starke U, Batteas J D, Van Hove M A and Somorjai G A 1994 *Surf. Sci.* **303** 319
[93] Batteas J D, Barbieri A, Starkey E K, Van Hove M A and Somorjai G A 1994 *Surf. Sci.* **313** 341
[94] Van Hove M A 1994 *Surf. Rev. Lett.* **1** 9
[95] Barbieri A, Van Hove M A and Somorjai G A 1994 *Surf. Sci.* **306** 261
[96] Barbieri A, Weiss W, Van Hove M A and Somorjai G A 1994 *Surf. Sci.* **302** 259
[97] Weiss W, Barbieri A, Van Hove M A and Somorjai G A 1994 *Phys. Rev. Lett.* (submitted)
[98] Materer N, Starke U, Barbieri A, Van Hove M A and Somorjai G A 1994 *Phys. Rev. Lett.* (submitted)
[99] Hu P, Wander A, Delagarza L M, Bessent M P and King D A 1993 *Surf. Sci.* **286** L542
[100] Urano T, Hongo S and Kanaji T 1993 *Surf. Sci.* **287/288** 294
[101] Liu W, Lai J R and Mitchell K A R 1993 *Surf. Sci.* **281** 21